Mol. Cells *32*, 89-98, July 31, 2011
DOI/10.1007/s10059-011-1048-9

Molecules and Cells

©2011 KSMCB

Septin 6 Regulates the Cytoarchitecture of Neurons through Localization at Dendritic Branch Points and Bases of Protrusions

Sun-Jung Cho[1,3], HyunSook Lee[1], Samikshan Dutta[1], Jinyoung Song[1,4], Randall Walikonis[2], and Il Soo Moon[1,*]

Septins, a conserved family of GTP-binding proteins with a conserved role in cytokinesis, are present in eukaryotes ranging from yeast to mammals. Septins are also highly expressed in neurons, which are post-mitotic cells. Septin6 (SEPT6) forms SEPT2/6/7 complexes *in vivo*. In this study, we produced a very specific SEPT6 antibody. Immunocytochemisty (ICC) of dissociated hippocampal cultures revealed that SEPT6 was highly expressed in neurons. Developmentally, the expression of SEPT6 was very low until stage 3 (axonal outgrowth). Significant expression of SEPT6 began at stage 4 (outgrowth of dendrites). At this stage, SEPT6 clusters were positioned at the branch points of developing dendrites. In maturing and mature neurons (stage 5), SEPT6 clusters were positioned at the base of filopodia and spines, and pre-synaptic boutons. Detergent extraction experiments also indicated that SEPT6 is not a post-synaptic density (PSD) protein. Throughout morphologic development of neurons, SEPT6 always formed tiny rings (external diameter, ~0.5 μm), which appear to be clusters at low magnification. When a Sept6 RNAi vector was introduced at the early developmental stage (DIV 2), a significant reduction in dendritic length and branch number was evident. Taken together, our results indicate that SEPT6 begins to be expressed at the stage of dendritic outgrowth and regulates the cytoarchitecture.

INTRODUCTION

Septins, a conserved family of GTP-binding proteins, are present in eukaryotes ranging from yeast to mammals, and have a conserved role in cytokinesis and/or cell septation. Septins were originally identified in mutant *Saccharomyces cerevisiae* that exhibit cell cycle arrest and aberrant bud growth (Hartwell, 1971; Hartwell et al., 1970; 1974). In yeast, septins are recruited to the incipient site of bud growth where they polymerize to form a network of highly ordered filaments (septin rings; Byers and Goetsch, 1976; Hartwell, 1971; Longtine et al., 1996; Oh and Bi, 2011). The septin ring at the mother-bud neck has two main functions. First, the septin rings serves as a scaffold for protein-protein interactions to recruit selective proteins at the site (Douglas et al., 2005; McMurray and Thorner, 2009). Second, septin rings function as a diffusion barrier across the plane of the mother-bud neck (Caudron and Barral, 2009). To date, 14 mammalian septin genes (SEPT1-14) have been identified (Cao et al., 2009; McMurray and Thorner, 2009). As protein scaffolds and diffusion barriers, septins have conserved their key roles in cell polarity and cell-cycle progression (Gladfelter et al., 2001; Kinoshita, 2006; Longtine and Bi, 2003; McMurray and Thorner, 2009; Park et al., 2010).

Neurons are highly polarized cells with complex branching in the dendrite and axon. A neuronal dendrite is further polarized to produce extensive protrusions, the so-called spines. By mass spectrometric analysis, 9 of 14 septins (SEPT2-9, and SEPT11) have been identified in rat brain spines (Collins et al., 2005; Hall et al., 2005; Peng et al., 2004). The functions of neuronal septins have been elusive because septin-deficient mice have shown normal neuronal development (SEPT3, Fujishima et al., 2007; SEPT4, Ihara et al., 2005; SEPT5, Peng et al., 2002; SEPT6, SEPT6/SEPT4, SEPT11, Ono et al., 2005). However, observations of septin-downregulated neurons in culture have shown subtle alterations in the cytoarchitecture of dendritic arborization and spines (SEPT2, 5-7, Tada et al., 2007; Xie et al., 2007; SEPT11, Li et al., 2009). Changes in behavior have also been reported. Suzuki et al. (2009) showed that a SEPT5 deficiency exerts pleiotropic effects on a select set of affective behaviors and cognitive processes depending on the genetic background.

SEPT6 is expressed in all tissue types, but shows high expression in lymphoid tissues (with SEPT1, 9, and 12, Hall et al., 2005). SEPT6-deficient and SEPT6/SEPT4-deficient mice do not exhibit gross abnormalities, changes in cytokinesis, spontaneous malignancy, or neurologic disorders (Ono et al., 2005).

[1]Department of Anatomy, College of Medicine, Dongguk University, Gyeongju 780-714, Korea, [2]Department of Physiology and Neurobiology, University of Connecticut, CT 06269, USA, [3]Present address: Division of Brain Diseases, Center for Biomedical Sciences, National Institute of Health, Osong Health Technology Administration Complex, Cheongwon 363-951, Korea, [4]Present address: Department of Pediatrics, Sejong General Hospital, Bucheon 422-711, Korea
*Correspondence: moonis@dongguk.ac.kr

Received March 11, 2010; revised April 4, 2011; accepted April 6, 2011; published online May 2, 2011

Keywords: dendrite, filopodia, microtubule, RNAi, septin 6, spine

However, using cultured rat hippocampal neurons Xie et al. (2007) have shown that overexpression of SEPT6 increased the density of dendritic protrusions, while knockdown of SEPT6 by RNA interference (RNAi) significantly reduced protrusion density, and the remaining protrusions were on average slightly longer and wider. Information on the subcellular expression of SEPT6 is limited. Nine of 14 septins (SEPT2-9 and SEPT11, including SEPT6) have been found in rat brain post-synaptic density (PSD) fractions by mass spectrometry (Collins et al., 2005; Hall et al., 2005; Peng et al., 2004). In contrast, there have been two reports (Tada et al., 2007; Xie et al., 2007) that indicated SEPT6 at other than PSD fractions. It has been shown that SEPT7 localizes at the dendritic branch points, and at the base of filopodia and spines in developing hippocampal neurons in culture. Because SEPT6 forms a complex with SEPT2 and SEPT7 (SEPT2/6/7) *in vivo* (Kinoshita et al., 2002; Sheffield et al., 2003), it can be inferred that SEPT6 is also localized at those subcellular sites. However, due to a lack of specific antibodies, a detailed study on the expression of SEPT6 at the subcellular level is not possible. In this study we raised a very specific antibody against SEPT6. Using a highly specific affinity-pure antibody, we studied the developmental expression of SEPT6 in cultured hippocampal neurons. We have shown that significant level of SEPT6 expression begins only from developmental stage 4 (dendritic outgrowth) by forming tiny rings on microtubule fibers, and that SEPT6 positions include the branching point of developing dendrites and the base of dendritic protrusions (filopodia and spines) and axonal boutons. We further showed by RNAi experiments that SEPT6 regulates dendritic arborization.

MATERIALS AND METHODS

Antibodies

The following antibodies were used at the indicated dilutions: mAb gephyrin (Geph, clone 7a, 1:1000; Synaptic Systems, Germany) and mAb glycine receptor (GlyR, clone mAb4a, 1:500; Synaptic Systems); mAb actin (actin, 1:2000; Developmental Studies Hybridoma Bank, University of Iowa, USA); mAb tubulin α-subunit (Tub, 1:2000; Developmental Studies Hybridoma Bank); and mAb synaptic vesicle protein 2 (SV2, 1:1000; Developmental Studies Hybridoma Bank); mAb PSD-95 (PSD95; Upstate Biotechnology Inc., USA), *N*-methyl-*D*-amino acid receptor subunit 2A (NR2A; Upstate Biotechnology Inc.), and NR2B (1:1000; Upstate Biotechnology Inc.); chicken polyclonal PSD-95 (1:1000, antiserum UCT-C1, Murphy et al., 2006); and rabbit polyclonal affinity-pure septin6 (SEPT6; 1:1000, this work).

Subcellular fractionation and detergent extraction

One-Triton PSD fractions (Cho et al., 1992; Moon et al., 1994) were prepared from adult rat (~250 g, Sprague-Dawley) forebrains by washing synaptosome-enriched fractions with 0.5% Triton X-100, as previously described (Carlin et al., 1980; Cho et al., 1992). In detergent extraction experiments, One-Triton PSD fractions were extracted again at 4°C with 1.0% Triton or 1.0% n-octyl glucoside (OG) for 15 min or with 3% *N*-lauroylsarcosine [sarcosyl (Sarc)] for 10 min. Thereafter, the pellet and supernatant were separated by centrifugation at 201,800 $\times$ *g* for 1 h at 4°C, and the pellet was resuspended in 40 mM Tris-HCl (pH 8.0).

Preparation of antibodies against SEPT6

The C-terminal portion of rat SEPT6 was used to generate rabbit polyclonal antisera. The amino acid sequence of the peptide was GGSQTLKRDKEKKN, which corresponds to the C-terminus [residues 414-427 (SEPT6-C)]. The peptide was custom synthesized by Peptron, Inc. (Korea), purified by HPLC, and coupled to keyhole limpet hemocyanin via an added C-terminal cysteine and a succinimidyl 4-[N-malei-midomethyl] cyclohexane-1-carboxylate linker. The conjugate (500 μg/ml) was emulsified with an equal volume of Freund's complete adjuvant for the first immunization and with Freund's incomplete adjuvant for all subsequent immunizations. Two rabbits were injected at 2-week intervals. Antibody specificity was tested by pre-blocking with the indicated peptides. The antibody was purified using an immunoaffinity column that was constructed by cross-linking the SEPT6-C to iodoacetyl agarose. Affinity-purified anti-SEPT6 antibodies were used in all experiments.

Immunoblots

After separation by SDS-PAGE, proteins were transferred to nitrocellulose membranes. Blots were incubated overnight at 4°C in TTBS [0.2% Tween-20, 10 mM Tris-HCl (pH 7.5) and 0.2 M NaCl]. Primary antibody [affinity-purified rabbit polyclonal anti-SEPT6 (1:1,000; this work)] was added, and incubation was continued for ~2-4 h at room temperature. The blots were rinsed in TTBS (4 $\times$ 20 min), and the antigen-antibody complex was visualized using alkaline phosphatase-conjugated secondary antibodies, according to the manufacturer's instructions (Roche, Germany). For quantification, blots were scanned to acquire digital images. Signal intensities were measured using image analysis software (NIH Scion Image Beta 4.0.2) and are expressed as the mean $\pm$ standard deviation.

Neuronal culture and immunocytochemistry (ICC)

Hippocampi from Sprague-Dawley rat pups at embryonic day 18 (E18) or E19 were dissected, dissociated by trypsin treatment and mechanical trituration, and plated onto 12-mm diameter polylysine/laminin-coated glass coverslips at a density of ~150 neurons/mm^2 (Brewer et al., 1993). Cells were initially plated in Neurobasal medium supplemented with B27 (Invitrogen, USA), 25 μM glutamate, and 500 μM glutamine, and fed 5 days after plating, and weekly thereafter with the same media (without added glutamate) containing 1/3 (v/v) 'conditioned' Neurobasal media by incubating for 24 h on astrocyte cultures (Goslin et al., 1998). For immunocytochemistry, culture coverslips were rinsed briefly in Dulbecco's phosphate-buffered saline (D-PBS; Invitrogen), and the cells were fixed by a sequential paraformaldehyde/methanol fixation procedure (Moon et al., 2007). After pre-block, coverslips were incubated with primary, followed by secondary antibodies, and mounted on slides as described previously (Moon et al., 2007). Confocal images (1,024 $\times$ 1,024 pixels) were acquired using a 100X oil-immersion lens on a Leica TCS SP2 Confocal System with laser lines at 488, 543, and 633 nm, and processed with the use of Adobe Systems Photoshop 5.0 software.

RNA interference (RNAi)

An RNAi DNA template oligonucleotide (Sept6-si; 5′-CTGATA GATCTGGACTCC-3′) corresponding to 677~694 bp of *Rattus norvegicus* Sept6 mRNA (ref|NM_001173429.1|) and a control oligonucleotide (5′-CTC TTC GGA TCT TTA GCT C-5′) were designed. The efficacy of si-Sept6 was verified by Kremer et al. (2005). Sept6-si was as follows: sense, 5′-TTT GCG CTG ATA GAT CTG GAC TCC GTT GAT ATC CGC GGA GTC CAG ATC TAT CAG TTT TTT-3′; and antisense, 5′-CTA GAA AAA ACT GAT AGA TCT GGA CTC CGC GGA TAT CAA CGG AGT CCA GAT CTA TCA GCG-3′. The control was as follows:

sense, 5′-TTT GCG CTC TTC GGA TCT TTA GCT CTT GAT ATC CGG AGC TAA AGA TCC GAA GAG TTT TTT-3′; and antisense, 5′-CTA GAA AAA ACT CTT CGG ATC TTT AGC TCC GGA TAT CAA GAG CTA AAG ATC CGA AGA GCG-3′. Sense and antisense templates were annealed, and subcloned into the *Xba*I site of the mU6pro vector. Neurons were transfected using Lipofectamine™ 2000 reagents according to the manufacturer's instructions (Invitrogen).

Analysis

For co-localization analysis, SEPT6 clusters on branching points at the base of filopodia or spines from areas (50 μm × 50 μm; n = 10-15) of typical pyramidal neurons (n = 2-4) were counted, and expressed as a percentage of the total (mean ± SD). For dendritic arborization analysis, the number of primary dendrites at intersections on circles of 20, 30, and 40 μm diameter from the center of typical neurons were counted. Statistical significance was assessed by Mann-Whitney U-test. *p* values < 0.05 and 0.01 were considered to be significant and very significant, respectively.

RESULTS

Antibody specificity

A Blastp (protein-protein BLAST) search (as of 10 March 2011) of the SEPT6-C as a query revealed no other rat septins that have significant sequence identities with this peptide. Among the septins, the highest identities with the peptide was manually found in the SEPT11 C-terminus [identities = 8/14 (57%)]. The SEPT11 is composed of 425 amino acids, which is close to SEPT6 (427 aa). Therefore, the cross-reaction of our antibody with SEPT11 was tested by immunoblot analysis using antiserum and rat forebrain homogenate. As shown in Fig. 1A, the strongest immunoblot signals was detected at the 50 kDa position, of which size corresponded well to SEPT6 (Fig. 1A, arrowhead). To verify the 50 kDa band as SEPT6, we carried out antigen competition assays. When the SEPT6-C peptide (Fig. 1B) was added in the buffer, immunoblot signals at the 50 kDa position weakened in a dose-dependent fashion (Fig. 1A, arrowhead). In contrast, even a very high concentration of SEPT11-C peptide (Fig. 1B) did not weaken the 50 kDa band (Fig. 1A, lane 7). The inhibitory effect of SEPT6-C was very specific because no other signals were weakened (Fig. 1A, asterisk with a line). These results indicate that our antiserum contains an antibody very specific to SEPT6. Indeed, our affinity-pure SEPT6 antibody, which was purified from the antiserum using SEPT6-C, specifically recognized only one 50 kDa protein (Fig. 2). All of the following experiments were carried out using this affinity-pure antibody.

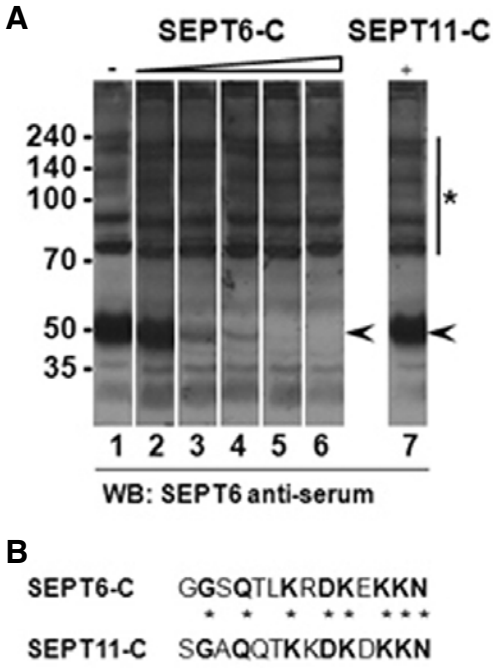

Fig. 1. Antibody specificity. (A) Immunoblots. Rat brain homogenate was electrophoresed in 8% SDS-gels, transferred to nitrocellulose, and immunoblotted with SEPT6 antiserum in the presence of variable concentration of competition peptides. Lane 1, antiserum only (1:1,000); lanes 2-6, antiserum (1:1,000) plus 0.0001, 0.001, 0.05, 0.1, 1.0, and 20 μg/ml of SEPT6-C, respectively; lane 7, antiserum (1:1,000) plus 20 μg/ml of SEPT11-C. The position of SEPT6 band and other nonspecific bands were marked with arrowheads and a bar with an asterisk. The molecular sizes are shown at far left in kilodaltons (kDa). (B) Sequence comparison between SEPT6-C and SEPT11-C. Identical amino acids are shown in bold and marked with asterisks.

SEPT6 is enclosed in the synaptosome, but not associated with the PSD

Densitometric analyses of Coomassie-stained protein bands indicated that the 50 kDa protein, which was identified as SEPT6 by amino acid sequencing (data not shown), represented a minor (~1.5%) protein in the One-Triton PSD fraction (Fig. 2A). Immunoblots revealed that the amount of SEPT6 increased in the synaptosome (Syn) and PSD fractions by 137 ± 18% (n = 3) and 162 ± 23% (n = 3), respectively (Fig. 2Ba). This enrichment was not significant when compared to PSD markers, such as NR2A, NR2B, and PSD-95 (Fig. 2Bb). To gain further insight into the relationship between SEPT6 and PSD we carried out detergent extraction experiments. Although mild non-ionic detergents OG (1.0%) and Triton X-100 (Triton, 1.0%) were not efficient in solubilizing SEPT6 (~10% and ~30%, respectively, n = 4; Fig. 2C), a harsh detergent sarcosyl (Sarc, 3%), and salt (1.0 M NaCl) solubilized SEPT6 almost completely (~98% and ~92%, respectively, n = 4; Fig. 2C, Sarc). Because 'core' PSD proteins are highly resistant to detergent extraction, these results indicate that SEPT6 is not a constituent of the PSD 'core.' In addition, the fact that SEPT6 is included in the synaptosome, but not significantly enriched in the PSD fraction suggests that it is located at the base of spines, or that it is included by contamination in the PSD fraction, which is highly sticky.

SEPT6 is highly expressed, and forms rings in neurons

To determine the pattern of SEPT6 expression in neurons, rat hippocampal dissociate cultures were subjected to ICC. Neurons exhibited a stronger SEPT6 immunoreactivity (IR; Fig. 3A, SEPT6, arrowheads) than oligodendrocytes and astrocytes (boxes a and b, respectively, in Fig. 3A). Under low-magnification micrographs of neurons, the SEPT6-IR showed a punctate distribution in association with microtubule fibers (Fig. 3B, left panel). To determine whether or not the SEPT6 clusters in the low magnification are actually rings, high resolution ICC confocal images were obtained from day 21 *in vitro* (DIV 21) neurons using a 100X objective lens in 4X digital magnification. Surprisingly, at this high resolution, the SEPT6-IR revealed ring or crescent shapes (external diameter ~0.5 μm; Fig. 3B, inset a). SEPT6-IR rings were also seen in young neurons (DIV 7),

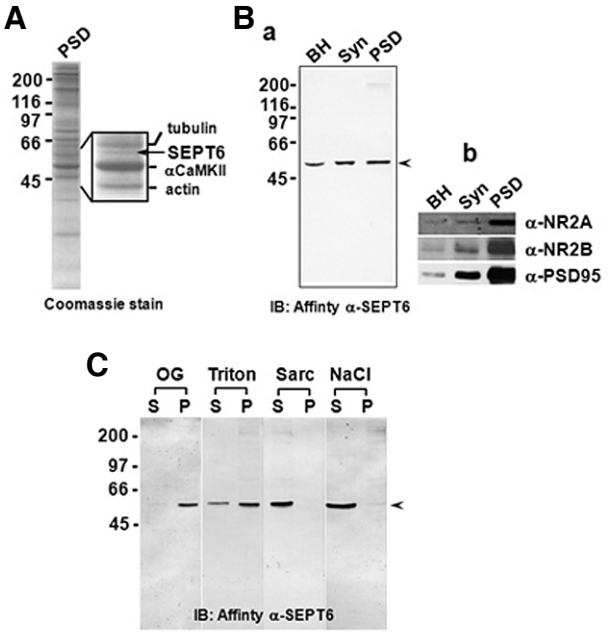

Fig. 2. SEPT6 is not a PSD protein of the rat forebrain. (A) A Coomassie-stained gel showing SEPT6 in the rat forebrain PSD fraction. The rat forebrain One-Triton PSD fraction was separated on a 10% SDS gel and stained with Coomassie blue R-250. The portion of the gel including the SEPT6 (arrow) was enlarged and shown along with identified proteins (inset). (B) Immunoblots showing no enrichment of SEPT6 in the PSD fraction. Forty micrograms of brain homogenate (BH), synaptosome (Syn), and One-Triton PSD (PSD) fractions were immunoblotted with affinitiy-pure rabbit polyclonal anti-SEPT6 (a). Control immunoblots for proteins known to enrich in the PSD were shown (b). (C) Detergent extraction experiments showing no inclusion of SEPT6 in the PSD 'core'. One-Triton PSD fractions were extracted with n-octyl-β-D-glucoside (OG, 1.0%), Triton X-100 (Triton, 1.0%), sarcosyl (Sarc, 3.0%), and NaCl (1.0 M). Soluble (S) and insoluble pellet (P) fractions were separated by centrifugation and immunoblotted with affinity-pure anti-SEPT6. The positions of SEPT6 were marked by arrowheads. Molecular sizes (in kDa) are indicated on the left of each panels.

indicating that SEPT6 forms rings in neurons, regardless of the developmental stages (Fig. 3B, inset b). These results show that SEPT6 is highly expressed and forms rings in neuronal soma and dendrites.

Significant expression of SEPT6 begins with extensive development of dendrites (developmental stage 4; dendritic outgrowth)

We next investigated the developmental expression of SEPT6. As shown in Fig. 4, SEPT6-IR signals were very low until stage 3. A significant SEPT6-IR was detected only after stage 4 when an extensive dendritic development occurs (Fig. 5). This result indicates that SEPT6 does not play a major role in the initial development of minor processes (stage 2) and axonal development (stage 3), but implies that it plays an important role in the dendritic development (stage 4 and later).

SEPT6 positions at branching points and the bases of filopodia of developing dendrites

Significant SEPT6-IR clusters appeared in the somatodendritic domain of stage 4 neurons (Fig. 5A). At this stage of morphol

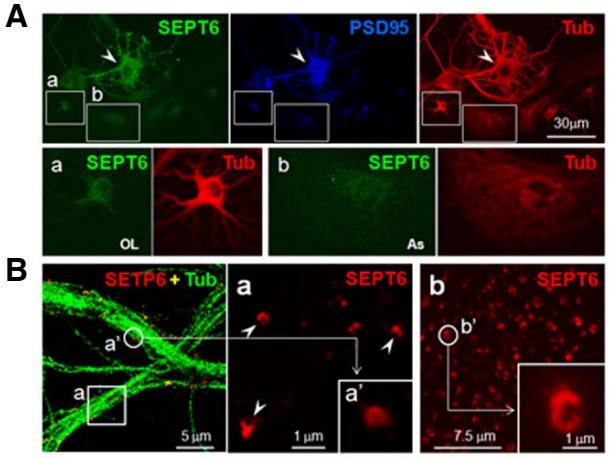

Fig. 3. SEPT6 is highly expressed, and forms rings in neurons. (A) Confocal microscopic images showing high expression of SEPT6 in neurons. Rat hippocampal dissociate cultures (DIV 21) were triple-labeled by ICC with anti-SEPT (green), -PSD-95 (blue), and -tubulin (Tub; red). The boxed area *a* (oligodendrocyte; OL) and (b) (astrocyte; As) were shown enlarged at the bottom. A neuron is marked by an arrowhead. Scale bar, 30 μm. (B) Confocal micrographs showing SEPT6 rings. Left, A merge of SEPT6 (red) and Tub (green) was shown. Scale bar, 5.0 μm. The SEPT6 image of the boxed area *a* was shown enlarged on the right. One SEPT6-IR cluster (a′) was enlarged in the inset of (a) to show the ring structure. Some SEPT6-IR's of ring or crescent shapes were marked by arrowheads. Scale bar, 1.0 μm. In (b), a portion of dendrites of a developing neuron (stage 4) was shown after immunostaining with anti-SEPT6. Scale bar, 7.5 μm. One SEPT6 cluster (b′) was enlarged to show ring or crescent shapes. Scale bar of the inset, 1.0 μm.

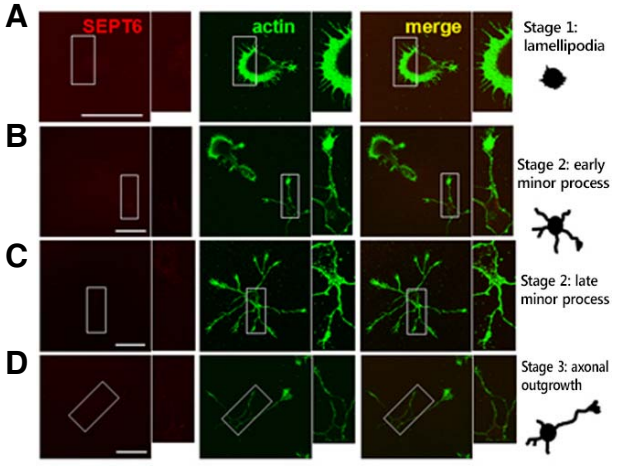

Fig. 4. ICC showing no significant expression of SEPT6 in the early neuronal development. Confocal microscopic images showing rat hippocampal neurons in culture at developmental stage 1 [lamellipodia; (A)], early and late stage 2 [minor processes; (B and C), respectively], and stage 3 [axonal outgrowth; (D)]. Cells were double-labeled with anti-SEPT6 (red) and -pan actin (green). Boxed areas are shown enlarged in insets. Drawings for typical neurons at each stage are shown at far right (Dotti et al., 1988). Scale bar, 30 μm.

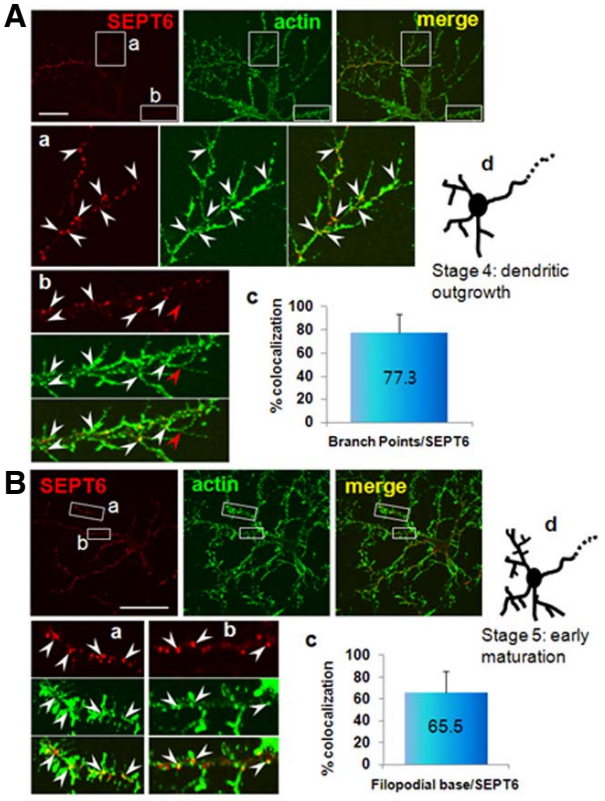

Fig. 5. Confocal microscopic images showing expression of SEPT6 in maturing dendrites. Rat hippocampal neurons in culture were double-labeled with anti-SEPT6 (red) and -pan actin (green). (A) Developmental stage 4 (dendritic outgrowth; DIV 7 for this particular neuron). Boxed area (a) and (b) are shown enlarged at the bottom [(a) and (b), respectively]. Some branching points which have SEPT6 clusters are marked by arrowheads. (c) Statistics. The percentage of the branching point with SEPT6 is shown. (d) Schematic drawing of a typical neuron at stage 4 (Dotti et al., 1988). Scale bar, 30 μm. (B) Early developmental stage 5 (maturation; DIV 14 for this particular neuron). A neuron in early dendritic maturation is shown. Annotations are the same as in (A). Note that most dendritic protrusions are long and thin, the features of filopodia (a), and that some are short and stubby, the features of spines (b).

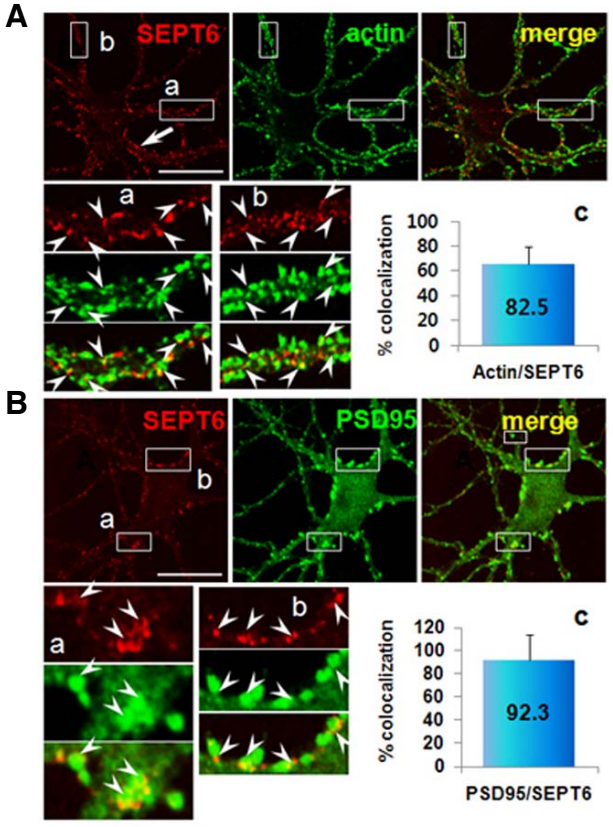

Fig. 6. Confocal microscopic images showing localization of SEPT6 at the base of spine. Rat hippocampal neurons in culture (DIV 21) were double-labeled with anti-SEPT6 (red) and spine markers, -pan actin [(A); green] or PSD-95 [(B); green]. Annotations are the same as Fig. 4A. Note semi-circular appearance of SEPT6-IR (inset a of B) and positioning of SEPT6-IR at the base of spines.

ogic development, the density of SETP6 clusters was low (~6 ea/20 μm; Fig. 5A, SEPT6) as compared to mature neurons (~20 ea/20 μm; Fig. 6, SEPT6). To find the relative positions of these SETP6 clusters in the developing branches, the contour of dendrites was revealed by double-labeling the stage 4 neurons with SEPT6 and pan-actin antibodies (Fig. 5A, actin). In both distal tertiary (inset a) and proximal primary (inset b) dendrites, most (77 ± 16%) of the SEPT6-IR clusters were positioned at the branching points. Next, we analyzed the position of SEPT6-IR clusters in relation to filopodia of early maturing neurons (Fig. 5B). Two dendritic regions were shown to be enlarged, as follows: one region with a relatively longer protrusion (inset a) and the other region with a shorter (inset b) protrusion. The majority (65 ± 20%) of the filopodia had SEPT6-IR clusters at the base or neck (Fig. 5B). These results suggest that SEPT6 plays important roles in dendritic branching and protrusions.

SEPT6 forms rings at the neck of spines

To investigate the subcellular localization of SEPT6 in mature neurons, we double-labeled hippocampal neurons (DIV 21) with antibodies directed against SEPT6 and actin. The confocal microscopic images showed dense (~20 ea/μm) and strong SEPT6-IR clusters in dendrites (Fig. 6A, SEPT6). The positions of these clusters were not randomly distributed in dendrites, but concentrated at the periphery. This feature was most evident in large dendrites (Fig. 6A, SEPT6, arrow). The actin-IR was also punctate along the periphery of dendrites (Fig. 6A, actin). In neurons, F-actin is particularly enriched in dendritic spines (Cohen et al., 1985; Matus et al., 1982; Sekino et al., 2007). Therefore, actin-IR clusters in dendritic protrusions are mostly spines in mature neurons. SEPT6- and actin-IR merge images revealed that the majority of SEPT6 clusters (82 ± 14%, counted actin cluster no. = 212) was juxtaposed with actin, such that actin clusters were positioned peripheral to SEPT6 in the dendritic shaft (Fig. 6A, insets a, b). This feature suggests that SEPT6 is positioned at the base of dendritic spines.

To confirm the positioning of SEPT6 at the base of spines, we double-labeled a sister hippocampal neuronal culture with SEPT6 and PSD-95, a marker for excitatory a post-synaptic membrane (i.e., PSD fraction; Cho et al., 1992). The confocal microscopic images showed robust PSD-95-IR clusters along the periphery of dendrites, often protruding out (Fig. 6B, PSD95). Statistical analysis showed that 92 ± 22% of PSD-95

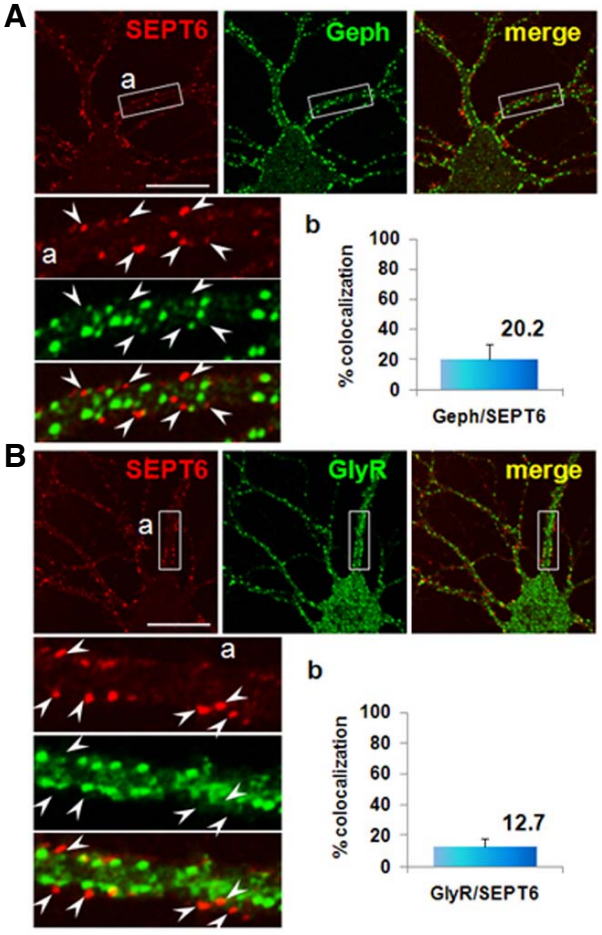

Fig. 7. Localization of SEPT6 is very low in the inhibitory postsynaptic sites. Rat hippocampal neurons in culture (DIV 21) were double-labeled with anti-SEPT6 (red) and -gephyrin [Geph, (A); green] or -glycine receptor [GlyR, (B); green], inhibitory synaptic markers. Annotations are same as Fig. 4A. Note that SEPT6 clusters are well separated toward periphery from those of inhibitory postsynaptic sites, which are positioned centrally relative to SEPT6.

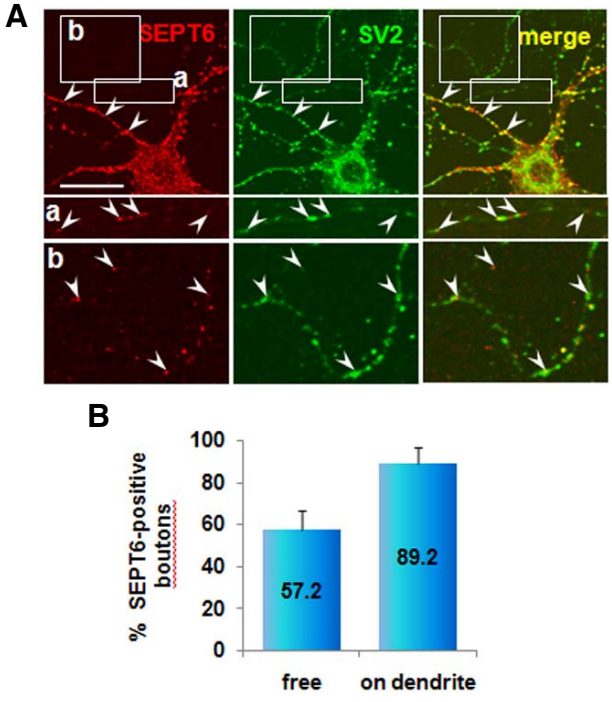

Fig. 8. Confocal microscopic images showing localization of SEPT6 at the axonal boutons. Rat hippocampal neurons in culture (DIV 21) were double-labeled with anti-SEPT6 (red) and SV2, a marker for synaptic vesicles (A) Pre-synaptic terminals on dendrites are marked with arrowheads. The free boutons en passant [box (a) and (b)] are shown at bottom in high contrast and marked with arrowhead. Statistics of boutons positive for SEPT6 is shown in percentage (B) Scale bar, 30 μm.

(+) protrusions (counted PSD-95 clusters = 254) juxtaposed with SEPT6 (touching each other or partially overlapping). The high resolution images were shown enlarged in insets a and b. Inset a, which represents spines protruding in the *z*-axis, shows ring-shaped SEPT6-IR clusters in the head-to-neck facet. Instead, inset b, which represents spines protruding in the X-Y plane, shows dot-like split clusters at each side of the spine bases. In the latter examples, positioning of SEPT6 at the neck/base of the spine was very clear.

Low co-localization of SEPT6 with inhibitory post-synaptic markers

To investigate the relationship between SEPT6 and inhibitory post-synaptic sites, we double-labeled hippocampal neurons (DIV 21) with antibodies directed against SEPT6 and Geph or GlyR. Gephyrin is a major component of type II GABAergic and glycinergic synapses (Fritschy et al., 2008; Kneussel and Loebrich, 2007; Luscher and Keller, 2004). The Geph-IR clusters were positioned mostly at the periphery of dendritic shafts (Fig. 7A, Geph). However, when the positions of SEPT6 and Geph were compared, SEPT6 were further toward the periphery of dendritic shafts (Fig. 7A, merge). This feature is in contrast to the case of spine markers (actin- and PSD-95-IR). Merging of SEPT6 and Geph images showed that the two IR clusters did not juxtapose well. Only 20 ± 10% (number of counted Geph-IR clusters = 665) of Geph-IR clusters neighbored those of SEPT6. A very similar trend of spatial positioning was shown in the merged image of GlyR- and SEPT6-IR, SEPT6 being further toward the periphery (Fig. 7B). The juxtaposing rate of SEPT6/GlyR was only 13 ± 5% (number of counted GlyR-IR clusters = 390). These results suggest that SEPT6 is preferentially localized to excitatory post-synaptic sites.

SEPT6 is present in the pre-synaptic terminal and boutons en passant

To determine the presence of SEPT6 in the axon terminal we double-labeled hippocampal neurons (DIV 21) with antibodies directed against SEPT6 and SV2 (a synaptic vesicle protein). The SEPT6-IR signal was negligible in axonal shafts (Fig. 8A). However, variable intensities in IR signals for both SEPT6 and SV2 antibodies were associated with axonal boutons (Fig. 8A). In general, both IR signals of axonal boutons touching dendrites were strong (Fig. 8A, arrowheads), while IR signals of free boutons en passant were weak (Fig. 8A, insets a and b). Most of the axonal boutons on dendrites strongly expressed SEPT6 (89.2 ± 7.2%; number of counted SV2-IR boutons = 102; Fig. 8B, on dendrite). In contrast, both IR signals were very weak with the free boutons en passant. However, high-contrast images revealed about one-half (57.2 ± 9.5%; no. of counted SV2-IR boutons = 83) expressing SEPT6. These re-

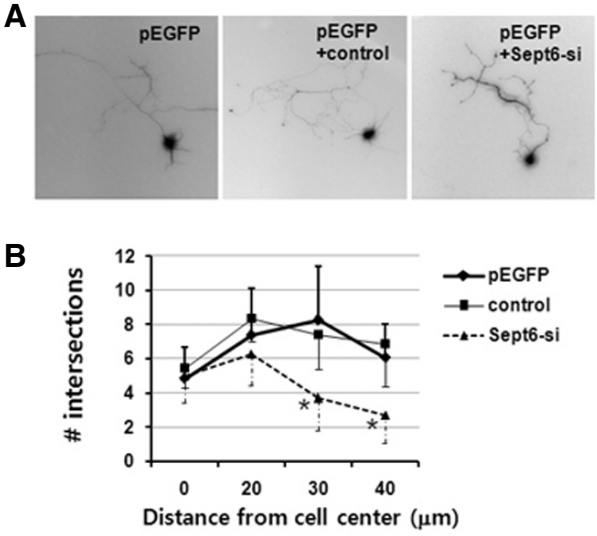

Fig. 9. SEPT6 RNAi impairs dendritic arborization. E18 rat hippocampal neurons were dissociated, transfected on DIV 2, and further incubated for 3 days. (A) Typical images of neurons transfected with pEGFP only, pEGFP+control oligonucleotide vector, and pEGFP+Sept6 RNAi vector (Sept6-si). (B) Statistics. Dendrite complexity of neurons was measured by Sholl analysis, which shows the number of dendrites crossing circles (vertical axis) at various radial distances from the center of cell soma (horizontal axis). *, $p < 0.01$.

sults suggest that SEPT6 is recruited to pre-synaptic boutons as the boutons mature developmentally or in a synaptic activity-dependent manner.

SEPT6 knockdown in the early developmental stage impairs dendritic development

To gain insight on the function of SEPT6, we introduced small interference RNA (RNAi) into developing neurons. A specific small hairpin RNA (shRNA)-expressing construct targeting Sept6 (Sept6-si) was generated using the mU6pro vector. Previously, this RNAi caused > 70% knockdown of SEPT6 when introduced in HeLa cells (Kremer et al., 2005). In our hands, RNAi also caused ~70% knockdown of SEPT6 when introduced in HEK293T cells (data not shown). The control construct, however, did not cause any knockdown. To determine the function of SEPT6 in dendritic development, we introduced Sept6-si vector in early developmental stages (before stage 4). A typical neuron that was transfected on DIV 2 (axonal outgrowth stage) with Sept6-si and grown 3 more days (dendritic outgrowth stage) was shown in Fig. 9A (pEGFP + Sept6-si). Apparently, the axonal growth was not affected. However, impairment in the dendritic growth was evident. When compared with neurons transfected with pEGFP and pEGFP + control construct, neurons that were transfected with pEGFP + Sept6-si exhibited a significant reduction in the dendritic length and branch number (Fig. 9B). There were no changes in the number of primary dendrites which protrude directly out of the soma. These results confirm that SEPT6 plays a critical role in dendritic development.

DISCUSSION

Our antibody specifically recognizes SEPT6

We have shown that our SEPT6 antibody was specifically 'muzzled' by its ortholog peptide. The SEPT11-C peptide, which has the highest identity to SEPT6, did not 'muzzle' the antibody, indicating it is very specific to SEPT6. Further indication for the specificity was derived from immunoblots. The affinity-pure SEPT6 antibody recognized only one band at 50 kDa in all BH, Syn, and PSD fraction lanes. SEPT11 has 80% identity in amino acid sequences and the molecular size (425 aa) is very close to SEPT6 (427 aa). Previous reports, however, showed that the two protein bands are resolved in SDS-PAGE. For example, the apparent molecular size of SEPT11 was 45 kDa in the human T-cell leukaemia cell line, JURKAT, and human umbilical vein endothelial cells (HUVECs; Bläser et al., 2006), and SEPT11 was slightly smaller than SEPT6 In COS7 cells (Ito et al., 2009). Therefore, if our antibody recognizes both SEPT6 and SEPT11, the two peptides may have been resolved in SDS-PAGE due to the difference in apparent molecular sizes. Furthermore, the SEPT11 rabbit polyclonal antibody raised using glutathione S-transferase-fused human SEPT11 C-terminal fragment (aa, 366-429) did not recognize SEPT6 (Hanai et al., 2004). This C-terminal fragment encompasses the region of our SEPT11-C peptide. Taken together, we conclude that our antibody is very specific to SEPT6.

SEPT6 is enclosed in the synaptosome fraction, but is not a PSD protein

Our data showed that SEPT6 is enclosed in the synaptosome and PSD fractions. However, SEPT6 was efficiently washed out from PSD fractions by salt and sarcosyl, to which 'core' PSD proteins, such as NR2A, NR2B, and PSD-95, are resistant. This phenomenon strongly indicated that SEPT6 is not a PSD protein. Indeed, ICC data showed that SEPT6 is located at the base of spines, but not at the head or post-synaptic membrane where the PSD fraction is located (SEPT6 and PSD95 double-label). Therefore, we conclude that SEPT6 is enclosed in the PSD fraction by contamination during fractionation. Similarly, six septins (SEPT2, 4-7, 11) were shown not to be enriched in the PSD fraction (Tada et al., 2007). Therefore, the septins, which were found in rat brain PSD fractions by mass spectrometry (Collins et al., 2005; Hall et al., 2005; Peng et al., 2004), are likely localized at the base of spines (SEPT5/7, Tada et al., 2007; SEPT11, Li et al., 2009).

The level of expression of SEPT6 in neurons at the early developmental stages is very low

We have shown that SEPT6 begins to be significantly expressed from the dendritic outgrowth stage (stage 4) and localizes at the branching point of dendritic arborization and at the base of filopodia and spines during neuronal maturation (stage 5). Hippocampal neurons in culture acquire a characteristic form by a stereotyped sequence of developmental events (Dotti et al., 1988). Shortly after the cells attach to the substrate, motile lamellipodia develop around the periphery of the cell (stage I: formation of lamellipodia). In the course of a few hours, the cells first establish several, apparently identical, short processes (stage 2: outgrowth of the minor processes). After several hours, one of the short processes begins to grow very rapidly and become the axon (stage 3: formation and growth of the axon). The remaining processes begin to elongate a few days later and grew at a much slower rate. The processes became the cell's dendrites (stage 4: growth of dendrites), and further dendritic arborization and spine formation follow (stage 5: maturation). The fact that SEPT6 is not significantly expressed until the axonal outgrowth occurs indicates that SEPT6 is not involved in the initial development of axon and dendrite. Very low expression at the early developmental stage is in

good agreement to the *in vivo* expression of SEPT6. Tada et al. (2007) showed that SEPT6 is highly expressed in the adult cortex and hippocampus. However, the level of expression of SEPT6 and SEPT7 was very low in the E18 cortex and hippocampus, and gradually increased as the brain developed. Neurogenesis in the cortical and hippocampal regions of the rat brain occurs between E14-E20 (Bayer and Altman, 1995). Therefore, the low expression of SEPT6 in the early stages of neuronal development observed in the present work corresponds well to the *in vivo* events.

SEPT6 is highly expressed and forms rings in neurons

Our results show that SEPT6 is highly expressed in neurons. The level of expression of SEPT6 in oligodendrocytes and astrocytes was much lower than in neurons. A relatively high expression of SEPT6 suggests an important role in neurons. We further showed that throughout neuronal development SEPT6-IR always forms clusters, which co-localize with microtubule fibers. We never encountered fiber-like SEPT6 structures in any developmental stages. The SEPT6 clusters were actually ring- or crescent-shaped (approximately 0.5 μm in external diameter) at the high magnification, and the SEPT6 rings were always located on microtubule fibers. This result indicates that SEPT6 forms separate rings along microtubule fibers in neurons in normal physiology. This finding was unexpected because it is known that septins in mammalian cells are in a linear organization along actin bundles, and cytoplasmic rings of approximately 0.6 μm in diameter, occurs only when actin bundles are disturbed (Kinoshita et al., 2002). However, recent studies have shown that many septins interact with the microtubule cytoskeleton (Silverman-Gavrila and Silverman-Gavrila, 2008). Specifically, SEPT6 localizes to spindles of MDCK and HeLa cells (Spiliotis et al., 2005). SEPT6 binds MAP4 and prevents binding to microtubules, thus reducing microtubule stability (Kremer et al., 2005). Therefore, a higher order of SEPT6 organization may depend on cell types and the specific functions.

SEPT6 localizes at the branching points and promotes branching and growth of developing dendrites

Significant expression of SEPT6 from stage 4 implies that SEPT6 plays important roles in dendritic development/maturation. At this stage, SEPT6 localizes at the branching points of dendrites, suggesting a role for SEPT6 in dendritic branching. It has been reported that SEPT7 localizes at the dendritic branch points, and at the base of filopodia and spines in developing hippocampal neurons in culture (Tada et al., 2007; Xie et al., 2007). Because SEPT7 is a member of SEPT2/6/7 complexes *in vivo* (Kinoshita et al., 2002; Sheffield et al., 2003), similarity in the subcellular distribution of SEPT6 and 7 is not surprising. Our SEPT6 knockdown experiments by RNAi have shown that SEPT6 promotes dendritic branching and growth. Previously, Tada et al. (2007) studied the function of SEPT2,5-7 using relatively more developed neurons, i.e., DIV 12 (transfected on DIV 7 and further grown for 5 days). It was reported that overexpression of these septins increased the number of dendritic branches, while knockdown by RNAi reduced the number of dendritic branches. In our case, we used DIV 2 cells for transfection to observe the effect of SEPT6 on the early development of dendrites and axons, and found that SEPT6 RNAi reduced the branch number and final length of dendrites.

SEPT6 localizes at the base of filopodia and forms ring-like structures at the neck of spines

Spine formation begins with extension of short, thin protrusions (filopodia). In this work, we have shown that SEPT6 localizes at the base of filopodia and spines in maturing dendrites. Because > 90% of excitatory axo-dendritic synapses occur on dendritic spines (Harris and Kater, 1994), our results indicate that SEPT6 localizes at the excitatory synaptic sites. In contrast, the juxtaposition rates (partial and entire overlap) of SEPT6 and inhibitory synaptic markers (Geph or GlyR) were very low (only 20 ± 10 and 13 ± 5%, respectively). Furthermore, SEPT6 typically positioned peripheral to inhibitory post-synaptic markers in dendritic shafts. This feature was in contrast to excitatory post-synaptic markers, which are positioned further peripheral to SEPT6. Together, these data indicate that SEPT6 is preferentially localized at the excitatory post-synaptic sites. Interestingly, high resolution confocal images of SEPT6 immunostaining showed ring-like structures at the base of spines. During this work we noticed that SEPT6-IR is always punctate in neurons throughout development. We did not encounter filamentous SEPT6-IR, indicating that SEPT6 do not polymerize into filaments in neurons under normal physiologic conditions. Instead, we showed here that SEPT6 forms a ring, which encircles the spine neck as a SEPT2/6/7 complex (Tada et al., 2007; Xie et al., 2007).

Positioning of SEPT6 at the base of dendritic protrusions explains its role in regulating the density and shape of spines. Overexpression and knockdown experiments have shown that SEPT6 (SEPT2 and SEPT6 as well) regulates the density of dendritic protrusions (Tada et al., 2007). In addition to the alteration in density, SEPT6 knockdown resulted in longer and wider protrusion, and abnormal branched and "spread" morphology of the spine head. It is likely that SEPT6 regulates traffic for peripheral and integral membrane proteins to and from dendritic protrusions. Therefore, a spine can be visualized as reminiscent of a bud of yeast, and the function of septins are conserved from yeast to mammals (Tada et al., 2007; Xie et al., 2007).

SEPT6 is present in the axonal boutons

Our data also indicate that SEPT6 accumulates in axonal boutons. However, the degree of SEPT6 accumulation was very different depending on the position of the boutons. Almost all axonal boutons touching dendrites strongly expressed SEPT6. In contrast, only one-half of the free boutons en passant weakly expressed SEPT6. An electron microscopic study by Konishita et al. (2000) also showed the pre-synaptic localization of SEPT6. Konishita et al. (2000) showed that SEPT6 is localized near the pre-terminal synaptic vesicles in the glomeruli and dendrodendritic synapses of olfactory bulbs, the striatum, and the cerebellar molecular layer. In our study, the SV2-IR signals of the free boutons en passant were weak, which is consistent with premature boutons. The SV2 is a component of all vertebrate synaptic vesicles (Buckley and Kelly, 1985), and the pre-synaptic accumulation of synaptic vesicles is a hallmark process in synaptic maturation (Garner et al., 2006). One mechanism for pre-synaptic vesicle clustering is the retrograde signaling via trans-synaptic adhesion molecules in contact with the post-synaptic structure (Scheiffele et al., 2000; Stan et al., 2010). Therefore, our data imply that SEPT6 accumulates in the axonal boutons as the boutons mature upon post-synaptic contact.

In conclusion, we produced a very specific antibody against SEPT6 and carried out high-resolution immunocytochemical imaging of cultured rat hippocampal neurons. Neurons expressed SEPT6 higher than astrocytes and oligodendrocytes. *In vitro* the expression of SEPT6 was low in early developmental stages (until stage 3: axonal outgrowth). Significant expression of SEPT6 began from stage 4, which is characterized by

outgrowth of dendrites. Throughout the morphologic development of neurons, SEPT6 did not form fibers. Instead, SEPT6 always formed tiny rings (external diameter, ~0.5 μm), which appear to be clusters at low magnification. In the developing neurons, SEPT6 was positioned at the dendritic branch points, at the base of filopodia, and spines. In mature neurons, SEPT6 localized to the spine neck and pre-synaptic terminal. SEPT6 RNAi caused significant impairment in dendritic arborization, such as reduction in dendritic length and branch number. Taken together, we conclude that SEPT6 regulates dendritic branching and protrusions; however, immunoelectron microscopic studies are necessary for more detailed localization of SEPT6.

ACKNOWLEDGMENTS

We thank Eun-jung Jung for technical assistance. This research was supported by the Basic Science Research Program through the National Research Foundation of Korea (NRF) funded by the Ministry of Education, Science and Technology (2010-0015982).

REFERENCES

Bayer, S.A., and Altman, J. (1995). Neurogenesis and neuronal migration. In The Rat Nervous System, 2nd ed., G. Paxinos, ed. (San Diego, USA: Academic Press Inc.), pp. 1041-1078.

Bläser, S., Röseler, S., Rempp, H., Bartsch, I., Bauer, H., Lieber, M., Lessmann, E., Weingarten, L., Busse, A., Huber, M., et al. (2006). Human endothelial cell septins: SEPT11 is an interaction partner of SEPT5. J. Pathol. *210*, 103-110.

Buckley, K., and Kelly, R.B. (1985). Identification of a transmembrane glycoprotein specific for secretory vesicles of neural and endocrine cells. J. Cell Biol. *100*, 1284-1294.

Byers, B., and Goetsch, L. (1976). A highly ordered ring of membrane-associated filaments in budding yeast. J. Cell Biol. *69*, 717-721.

Cao, L., Yu, W., Wu, Y., and Yu, L. (2009). The evolution, complex structures and function of septin proteins. Cell Mol. Life Sci. *66*, 3309-3323.

Carlin, R.K., Grab, D.J., Cohen, R.S., and Siekevitz, P. (1980). Isolation and characterization of postsynpatic densities form various brain regions: enrichment of different types of postsynaptic densities. J. Cell Biol. *86*, 831-843.

Caudron, F., and Barral, Y. (2009). Septins and the lateral compartmentalization of eukaryotic membranes. Dev. Cell *16*, 493-506.

Cohen, R.S., Chung, S.K., and Pfaff, D.W. (1985). Immunocytochemical localization of actin in dendritic spines of the cerebral cortex using colloidal gold as a probe. Cell. Mol. Neurobiol. *5*, 271-284.

Collins, M.O., Husi, H., Yu, L., Brandon, J.M., Anderson, C.N., Blackstock, W.P., Choudhary, J.S., and Grant, S.G. (2005). Molecular characterization and comparison of the components and multiprotein complexes in the postsynaptic proteome. J. Neurochem. *1* (Suppl), 16-23.

Dotti, C.G., Sullivan, C.A., and Banker, G.A. (1988). The establishment of polarity by hippocampal neurons in culture. J. Neurosci. *8*, 1454-1468.

Douglas, L.M., Alvarez, F.J., McCreary, C., and Konopka, J.B. (2005). Septin function in yeast model systems and pathogenic fungi. Eukaryot. Cell *4*, 1503-1512.

Fritschy, J.M., Harvey, R.J., and Schwarz, G. (2008). Gephyrin: where do we stand, where do we go? Trends Neurosci. *31*, 257-264.

Fujishima, K., Kiyonari, H., Kurisu, J., Hirano, T., and Kengaku, M. (2007). Targeted disruption of Sept3, a heteromeric assembly partner of Sept5 and Sept7 in axons, has no effect on developing CNS neurons. J. Neurochem. *102*, 77-92.

Garner, C.C., Waites, C.L., and Ziv, N.E. (2006). Synapse development: Still looking for the forest, still lost in the trees. Cell Tissue Res. *326*, 249-262.

Gladfelter, A.S., Pringle, J.R., and Lew, D.J. (2001). The septin cortex at the yeast mother-bud neck. Curr. Opin. Microbiol. *4*, 681-689.

Goslin, K., Assmussen, H., and Banker, G. (1998). Rat hippocampal neurons in low density culture. In Culturing Nerve Cells, 2nd ed., G. Banker and K. Goslin, eds. (Cambridge, MIT Press), pp. 339-370.

Hall, P.A., Jung, K., Hillan, K.J., and Russell, S.E. (2005). Expression profiling the human septin gene family. J. Pathol. *206*, 269-278.

Hanai, N., Nagata, K., Kawajiri, A., Shiromizu, T., Saitoh, N., Hasegawa, Y., Murakami, S., and Inagaki, M. (2004). Biochemical and cell biological characterization of a mammalian septin, Sept11. FEBS Lett. *568*, 83-88.

Harris, K.M., and Kater, S.B. (1994). Dendritic spines: cellular specializations imparting both stability and flexibility to synaptic function. Annu. Rev. Neurosci. *17*, 341-371.

Hartwell, L.H. (1971). Genetic control of the cell division cycle in yeast. IV. Genes controlling bud emergence and cytokinesis. Exp. Cell Res. *69*, 265-276.

Hartwell, L., Culotti, J., and Reid, B. (1970). Genetic control of the cell-division cycle in yeast. I. Detection of mutants. Proc. Natl. Acad. Sci. USA *66*, 352-359.

Hartwell, L.H., Culotti, J., Pringle, J.R., and Reid, B.J. (1974). Genetic control of the cell division cycle in yeast. Science *183*, 46-51.

Ihara, M., Kinoshita, A., Yamada, S., Tanaka, H., Tanigaki, A., Kitano, A., Goto, M., Okubo, K., Nishiyama, H., Ogawa, O., et al. (2005). Cortical organization by the septin cytoskeleton is essential for structural and mechanical integrity of mammalian spermatozoa. Dev. Cell *8*, 343-352.

Kinoshita, M. (2006). Diversity of septin scaffolds. Curr. Opin. Cell Biol. *18*, 54-60.

Kinoshita, A., Noda, M., and Kinoshita, M. (2000). Differential localization of septins in the mouse brain. J. Comp. Neurol. *428*, 223-239.

Kinoshita, M., Field, C.M., Coughlin, M.L., Straight, A.F., and Mitchison, T.J. (2002). Self- and actin-templated assembly of Mammalian septins. Dev. Cell *3*, 791-802.

Kneussel, M., and Loebrich, S. (2007). Trafficking and synaptic anchoring of ionotropic inhibitory neurotransmitter receptors. Biol. Cell *99*, 297-309.

Kremer, B.E., Haystead, T., and Macara, I.G. (2005). Mammalian septins regulate microtubule stability through interaction with the microtubule-binding protein MAP4. Mol. Biol. Cell *16*, 4648-4659.

Li, X., Serwanski, D.R., Miralles, C.P., Nagata, K., and De Blas, A.L. (2009). Septin 11 is present in GABAergic synapses and plays a functional role in the cytoarchitecture of neurons and GABAergic synaptic connectivity. J. Biol. Chem. *284*, 17253-17265.

Longtine, M.S., and Bi, E. (2003). Regulation of septin organization and function in yeast. Trends Cell Biol. *13*, 403-409.

Longtine, M.S., DeMarini, D.J., Valencik, M.L., Al-Awar, O.S., Fares, H., De Virgilio, C., and Pringle, J.R. (1996). The septins: roles in cytokinesis and other processes. Curr. Opin. Cell Biol. *8*, 106-119.

Luscher, B., and Keller, C.A. (2004). Regulation of GABAA receptor trafficking, channel activity, and functional plasticity of inhibitory synapses. Pharmacol. Ther. *102*, 195-221.

Matus, A., Ackermann, M., Pehling, G., Byers, H.R., and Fujiwara, K. (1982). High actin concentrations in brain dendritic spines and postsynaptic densities. Proc. Natl. Acad. Sci. USA *79*, 7590-7594.

McMurray, M.A., and Thorner, J. (2009). Septins: molecular partitioning and the generation of cellular asymmetry. Cell Div. *4*, 18.

Moons, I.S., Apperson, M.L., and Kennedy, M.B. (1994). The major tyrosine-phosphorylated protein in the postsynaptic density fraction is N-methyl-D-aspartate receptor subunit 2B. Proc. Natl. Acad. Sci. USA *91*, 3954-3958.

Moon, I.S., Cho, S.J., Jin, I., and Walikonis, R. (2007). A simple method for combined fluorescence in situ hybridization and immunocytochemistry. Mol. Cells *24*, 76-82.

Murphy, J.A., Jensen, O.N., and Walikonis, R.S. (2006). BRAG1, a Sec7 domain-containing protein, is a component of the postsynaptic density of excitatory synapses. Brain Res. *1120*, 35-45.

Oh, Y., and Bi, E. (2011). Septin structure and function in yeast and beyond. Trends Cell Biol. *21*, 141-148.

Ono, R., Ihara, M., Nakajima, H., Ozaki, K., Kataoka-Fujiwara, Y., Taki, T., Nagata, K., Inagaki, M., Yoshida, N., Kitamura, T., et al. (2005). Disruption of Sept6, a fusion partner gene of MLL, does not affect ontogeny, leukemogenesis induced by MLL-SEPT6, or phenotype induced by the loss of Sept4. Mol. Cell. Biol. *25*,

10965-10978.
Park, H.J., Park, H.W., Lee, S.J., Arevalo, J.C., Park, Y.S., Lee, S.P., Paik, K.S., Chao, M.V., and Chang, M.S. (2010). Ankyrin repeat-rich membrane spanning/Kidins220 protein interacts with mammalian Septin 5. Mol. Cells *30*, 143-148.
Peng, X.R., Jia, Z., Zhang, Y., Ware, J., and Trimble, W.S. (2002). The septin CDCrel-1 is dispensable for normal development and neurotransmitter release. Mol. Cell. Biol. *22*, 378-387.
Peng, J., Kim, M.J., Cheng, D., Duong, D.M., Gygi, S.P., and Sheng, M. (2004). Semiquantitative proteomic analysis of rat forebrain postsynaptic density fractions by mass spectrometry. J. Biol. Chem. *279*, 21003-21011.
Scheiffele, P., Fan, J., Choih, J., Fetter, R., and Serafini, T. (2000). Neuroligin expressed in nonneuronal cells triggers presynaptic development in contacting axons. Cell *101*, 657-669.
Sekino, Y., Kojima, N., and Shirao, T. (2007). Role of actin cytoskeleton in dendritic spine morphogenesis. Neurochem. Int. *51*, 92-104.
Sheffield, P.J., Oliver, C.J., Kremer, B.E., Sheng, S., Shao, Z., and Macara, I.G. (2003). Borg/septin interactions and the assembly of mammalian septin heterodimers, trimers, and filaments. J. Biol. Chem. *278*, 3483-3488.
Silverman-Gavrila, R.V., and Silverman-Gavrila, L.B. (2008). Septins: new microtubule interacting partners. Scientific World Journal *8*, 611-620.
Spiliotis, E.T., Kinoshita, M., and Nelson, W.J. (2005). A mitotic septin scaffold required for Mammalian chromosome congression and segregation. Science *307*, 1781-1785.
Stan, A., Pielarski, K.N., Brigadski, T., Wittenmayer, N., Fedorchenko, O., Gohla, A., Lessmann, V., Dresbach, T., and Gottmann, K. (2010). Essential cooperation of N-cadherin and neuroligin-1 in the transsynaptic control of vesicle accumulation. Proc. Natl. Acad. Sci. USA *107*, 11116-11121.
Suzuki, G., Harper, K.M., Hiramoto, T., Sawamura, T., Lee, M., Kang, G., Tanigaki, K., Buell, M., Geyer, M.A., Trimble, W.S., et al. (2009). Sept5 deficiency exerts pleiotropic influence on affective behaviors and cognitive functions in mice. Hum. Mol. Genet. *18*, 1652-1660.
Tada, T., Simonetta, A., Batterton, M., Kinoshita, M., Edbauer, D., and Sheng, M. (2007). Role of Septin cytoskeleton in spine morphogenesis and dendrite development in neurons. Curr. Biol. *17*, 1752-1758.
Xie, Y., Vessey, J.P., Konecna, A., Dahm, R., Macchi, P., and Kiebler, M.A. (2007). The GTP-binding protein Septin 7 is critical for dendrite branching and dendritic-spine morphology. Curr. Biol. *17*, 1746-1751.